Periodically forced leaky integrate-and-fire model

K. Pakdaman
Inserm U444, Faculté de Médecine Saint-Antoine, 27 Rue Chaligny, 75571 Paris Cedex 12, France
(Received 18 September 2000; revised manuscript received 8 January 2001; published 27 March 2001)

The discharge pattern of periodically forced leaky integrate-and-fire models is studied. While previous analyses have been mainly concerned with the response of this model to sinusoidal stimulation, our results hold for arbitrary periodic inputs. It is shown that, for any periodic input, the map representing the relation between input phases at consecutive discharge times can be restricted to a piecewise continuous, orientation preserving circle map. This implies that (i) the rotation number is well defined and independent of the initial condition, and (ii) in the same way as for sinusoidal forcing, other forms of periodic stimuli can evoke only one of four types of response, namely, phase locking, quasiperiodic discharges, nonchaotic aperiodic firing, and termination of the discharge after a finite number of firings.

DOI: 10.1103/PhysRevE.63.041907 PACS number(s): 87.10.+e, 05.45.Xt

The sinusoidally forced leaky integrate-and-fire model (LIFM) has been the topic of numerous investigations as a means for understanding the behavior of excitable and pacemaker cells [1–4]. The temporal evolution of the membrane potential of this model is governed by

$$\frac{dV}{dt} = -\frac{V}{\tau} + \mu + I(t) \quad \text{if} \quad V(t) < S_0,$$

$$V(t^+) = V_0 \quad \text{if} \quad V(t) = S_0, \tag{1}$$

where $V(t)$ is the membrane potential, S_0 the constant firing threshold, V_0 $(<S_0)$ the postdischarge resetting potential, τ the membrane time constant, $\mu\tau$ the resting potential, and $I(t)$ the periodic input signal with period $T=2\pi/\Omega$. Without loss of generality we assume that $\int_0^T I(t)dt=0$. The LIFM generates an action potential when V exceeds S_0, which is described by an impulse. After that, V is immediately reset to V_0. The process is repeated subsequently.

An important milestone in the analysis of the sinusoidally forced LIFM [i.e., $I(t)=A\sin(\Omega t+\theta)$] was set by Keener *et al.* [3]. These authors performed a careful study of the response to this specific input and showed that the LIFM can display one of four behaviors, and only these. That is, the model fires only transiently and remains quiescent henceforth, phase locks to the input, displays quasiperiodic discharges, or generates a nonchaotic irregular firing, with the last form of response occurring only for a measure zero range of forcing amplitudes and periods. In their analysis, they utilized the firing map describing the relation between consecutive firing times $t_n \mapsto t_{n+1} = f(t_n)$ [1]

$$f(t_n) = F^{-1}[F(t_n) + Se^{t_n/\tau}], \tag{2}$$

$$F(t) = e^{t/\tau}\left[\mu\tau - S + \frac{A\tau}{\sqrt{1+(\Omega\tau)^2}}\sin(\Omega t + \theta - \phi)\right], \tag{3}$$

where $\phi = \arctan(\Omega\tau)$, and the associated circle map $\theta_{n+1} = f_c(\theta_n) = f(\Omega t_n + \theta_n)[\mathrm{mod}\, 2\pi]$, where θ_n and θ_{n+1} are the phases of the periodic input at the firing times t_n and t_{n+1}.

Coombes and Bressloff [4] raised the interesting possibility for the LIFM to display several locked discharges with different rotation numbers for given parameter values (the rotation number is defined as the average number of firings per input cycle). While this is not possible when $I(t) = A\sin(\Omega t+\theta)$ [3], the issue remains unexplored for other classes of periodic forcing, in other words, there may exist one or several periodic inputs that elicit firings with different rotation numbers.

The main purpose of the present work is to investigate this issue. We show that for arbitrary periodic inputs the rotation number does not depend on the initial condition. To this end, we use an approach that is different from that of [3] in that, instead of using the explicit analytical expression of the solutions of Eq. (1), we focus on the geometrical properties of this equation. This enables us to generalize the analysis of sinusoidally forced LIF's not only to arbitrary periodic inputs, but also to a wider class of systems. An illustration of this latter point in a model for a mechanoreceptor neuron is given at the end of this paper.

Our key argument hinges upon establishing that, for any arbitrary periodic forcing I, the circle map f_c can always be restricted in such a way that it is piecewise continuous and orientation preserving. This point results from two properties of the following equation, which corresponds to Eq. (1) without resetting:

$$\frac{dx}{dt} = -\frac{x}{\tau} + \mu + I(t). \tag{4}$$

These two properties are (P1) if for $s>s'$ and some x_0, we have $-x_0/\tau+\mu+I(v)>0$ for all v in $[s,s']$, then $x(t,s,x_0)<x(t,s',x_0)$ for all t, where $x(t,s,x_0)$ represents the value at time t of the solution of Eq. (4) going through x_0 at time s, i.e., $t\to x(t,s,x_0)$ satisfies Eq. (4) with $x(s,s,x_0) = x_0$; (P2) the difference $x(t,s,x_0)-x(t,s,y_0)$ tends monotonically to zero as $t\to\infty$ for all x_0 and y_0.

The first property is shared by all scalar equations, and the second one results from the fact that the right hand side of Eq. (4) is a strictly decreasing function of x at fixed t. Therefore, all the results presented below hold in fact for the more general case

$$\frac{dV}{dt} = G(V,t), \quad V(t) \leqslant S_0,$$

$$V(t^+) = V_0 \quad \text{if} \quad V(t) = S_0, \tag{5}$$

where G is smooth, $G(V,\cdot)$ is periodic, and $G(\cdot,t)$ is strictly decreasing and changes sign.

We denote by $x^*(t)$ the unique T-periodic solution of Eq. (4) defined as $x^*(t) = \mu\tau + \int_{-\infty}^{t} I(s) e^{-(t-s)/\tau} ds$, and to which all other solutions $x(t)$ eventually converge. In the same way, we introduce $x^0(t)$, the ''x nullcline,'' as the x values such that $dx/dt = 0$, which is given by $x^0(t) = \mu\tau + \tau I(t + \theta/\Omega)$. Since dx/dt is a decreasing function of x, we have $dx/dt > 0$ whenever $x(t) < x^0(t)$, and $dx/dt < 0$ when $x(t) > x^0(t)$.

We show that the response of the LIFM to periodic stimulation is entirely determined by the relative positions of (the graphs of) x^* and x^0 with respect to the threshold S_0. To this end, we determine how these affect the circle map f_c, by considering the phases of the first discharge of solutions of Eq. (1) with initial conditions $V(t) = V_0$ for t in $[0,T]$.

We distinguish three parameter regions corresponding to three types of regimes and depending on the relative positions of x^* and x^0 with respect to the threshold S_0. These are presented below, with Fig. 1 summarizing the main points. In all panels of this figure, the thick solid line is $x^*(t)$, the dashed line $x^0(t)$, and the horizontal line at $x = 1$ the threshold S_0. The solid lines represent solution curves of Eq. (4), denoted by $x(t)$. The solutions $V(t)$ of Eq. (1) coincide with some $x(t)$ between two successive discharges, then undergo a jump to V_0 upon reaching the threshold (at the discharge time), and follow another solution $x(t)$ from that point on until the next firing.

(a) Region 1. $x^0(t) > S_0$, i.e., the dashed line is above the threshold (top panel in Fig. 1), which is equivalent to

$$-\frac{S_0}{\tau} + \mu + \min_t \{I(t)\} > 0. \tag{6}$$

Inequality (6) is equivalent to $-S_0/\tau + \mu + I(v) > 0$ for all $v \in [0,T]$. This in turn yields that $-V_0/\tau + \mu + I(v) > 0$. The fact that $x(t)$ increases monotonically as long as it is below $x^0(t)$, together with (P1) applied to the previous inequality, imply that (i) for any discharge t_n there is a unique consecutive discharge time t_{n+1}, and vice versa, and (ii) if $t_n > t_n'$ then $t_{n+1} > t_{n+1}'$. In other words, the map $f_c \;\; \theta_n \to \theta_{n+1}$ is an invertible orientation preserving circle map.

(b) Region 2. There are some u and v such that $x^0(u) < S_0$ and $x^*(v) > S_0$, i.e., the dashed line is not above the threshold and the thick solid line is not below it (second panel from the top in Fig. 1), which is equivalent to

$$-\tau \max_t \left\{ \int_{-\infty}^{t} I(s) e^{-(t-s)/\tau} ds \right\} < -\frac{S_0}{\tau} + \mu < -\min_t \{I(t)\}. \tag{7}$$

We consider the implications of these inequalities successively. The fact that the thick solid line is not below the

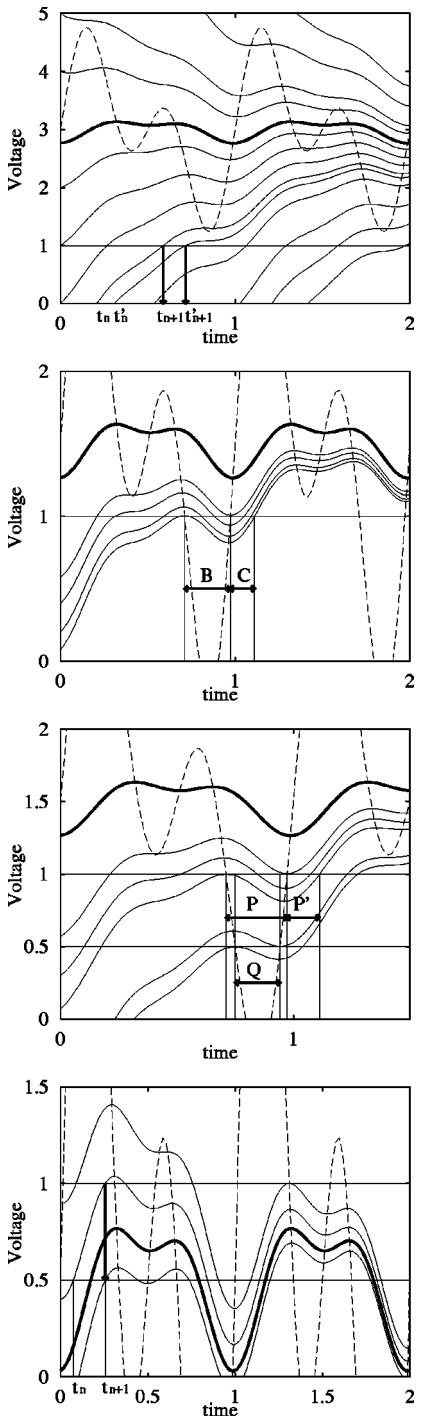

FIG. 1. All panels represent temporal wave forms of solutions $x(t)$ of Eq. (4). The thick solid line is the T-periodic solution $x^*(t)$, the dashed line represents the ''nullcline'' $x^0(t)$, and the horizontal line is the threshold S_0. The panels are representative examples of the dynamics in the different parameter regions 1, 2a, 2b, and 3 (see text for details). Abscissas of all panels are time and ordinates of all panels are voltage. Both quantities are expressed in arbitrary units. For all panels, the input is $I(t) = A\{\sin(2\pi t + \theta) + \sin(4\pi t + 2\theta)\}$. Parameters $S_0 = 1$, $V_0 = 0$, $\theta = 0$ rad, $A = 1$, and, top panel, $\mu = 3$, $\tau = 1$, second panel from top $\mu = 1.5$, $V_0 = -0.5$, third panel from top, $\mu = 1.5$, $V_0 = 0.5$, and bottom panel, $\mu = 0.5$, $V_0 = 0.5$, $A = 2$.

threshold [i.e., the left side inequality in (7)] ensures that the firing is sustained irrespective of the initial condition. In other words, for any s in $[0,t)$, there is some time $s'>s$ such that the solution of Eq. (4) satisfying $x(s)=V_0$ crosses the threshold at s'. This is due to the fact that $x(t)$ tends to $x^*(t)$, so that for some sufficiently large integer k $x(s+kT)>S_0$.

In the following we concentrate on the implications of the other condition, namely, that the dashed line is not above the threshold [i.e., the right side inequality in (7)]. To this end, we first consider the situation where the dashed line crosses the threshold, but remains above V_0 (second panel from the top in Fig. 1), and then we deal with the case when the dashed line crosses both S_0 and V_0 (third panel from the top in Fig. 1).

Region 2a. When $x^0>V_0$, (P1) implies that the map $t_n \to t_{n+1}$ is monotonic, or equivalently that f_c is orientation preserving. In this respect, the situation is similar to region 1. However, in contrast with that region, f_c is no longer invertible. This is because the solutions cannot reach the threshold from below at times such that $x^0(t)<S_0$ (e.g., the interval B in the second panel from the top in Fig. 1). In other words, such times do not belong to the range of f.

In fact, to be more accurate, defining $x(t,t_B,S)$ as the solution of Eq. (4) tangent to the threshold at the lower end t_B of B, it is the whole interval B-C wherein this solution remains below S that does not belong to the range of f, i.e., starting from V_0, it is not possible to cross the threshold from below and for the first time in this interval.

Region 2b. When x^0 crosses V_0, then $-V_0/\tau+\mu+I(v)<0$ for v in some interval (e.g., Q in the third panel from the top in Fig. 1). Then neither (P1) holds nor is the map f monotonic. To see this point, we consider an interval Q wherein x^0 is below V_0. We remark that there are two solution curves of Eq. (4) that are tangent to V_0 at each end of Q ($V_0=0.5$ in the figure). A solution $x(t)$ of Eq. (4) passing through V_0 to the left of Q, say at t_0 and enclosed between these two curves, crosses the horizontal V_0 line twice more, once from above within Q, say at t_0', and once from below to the right of Q, say at t_0'', with $t_0''>t_0'>t_0$. Since all these points are on the same solution curve $x(t)$, we have $f(t_0)=f(t_0')=f(t_0'')$, so that the map f is not one to one. Furthermore, for t and t' in Q, with $t>t'$, we have $f(t)<f(t')$, which means that f is locally decreasing in this interval, and hence its associated circle map f_c is not orientation preserving.

Nevertheless, we show that f restricted to its range is an increasing map, and its associated restricted circle map f_c is orientation preserving. To this end, we need only establish that intervals where f is not one to one—which include intervals such as Q—are not within the range of f. This is done in the following two paragraphs.

We first remark that Q wherein $-V_0/\tau+\mu+I(v)<0$ is necessarily strictly included in a larger interval P where $-S/\tau+\mu+I(v)<0$ because $S>V_0$. At the lower end t_p of P, there is a solution curve of Eq. (4) that is tangent to the threshold S, i.e., $t\to x(t,t_p,S)$ has a local maximum at $t=t_p$. This solution curve remains below S over an interval $P\cup P'$ which strictly contains P and crosses the threshold upward at t_p', with $t_p<t_p'$, i.e., $x(t_p',t_p,S)=S$ and $x(t,t_p,S)<S$ for all $t\in(t_p,t_p')$. No solution starting at V_0 can cross the threshold upward and for the first time within this interval $(t_p,t_p')=P\cup P'$. Therefore, this interval does not belong to the range of f.

To finish our proof, we have to show that this interval contains all points t_0' and t_0'' depicted above. Since Q is contained in P, we need only to establish that $t_0''<t_p'$. This results from (P2), i.e., the fact that the distance between any two solutions monotonically decreases with increasing time. More precisely, we remark that $x(t_0',t_p,S)-x(t_0',t_0',V_0)=x(t_0',t_p,S)-V_0<S-V_0$, because t_0' is in Q and consequently in P so that $x(t_0',t_p,S)<S$. Using (P2) and $t_p'>t_0'$, we obtain the result that $x(t_p',t_p,S)-x(t_p',t_0',V_0)<S-V_0$. Since, by definition, $x(t_p',t_p,S)=S$, we deduce that $x(t_p',t_0',V_0)>V_0$. This leads to $t_0''<t_p'$, because by definition $x(s,t_0',V_0)<V_0$ for all $s\in(t_0',t_0'')$.

(c) Region 3. $x^*(t)<S_0$, i.e., the thick solid line is below threshold (lowest panel of Fig. 1), which is equivalent to

$$-\frac{S_0}{\tau}+\mu+\tau\max_t\left\{\int_{-\infty}^{t} I(s)e^{-(t-s)/\tau}ds\right\}<0. \qquad (8)$$

All solutions of Eq. (4) eventually become completely subthreshold (e.g., the uppermost solid line in the lowest panel of Fig. 1). Let us consider one such solution, denoted by $x_M(t)$, that is above threshold in $[0,T]$, and let us denote by $t^*>T$ the last time it crosses the threshold. For $t>t^*$, this solution is subthreshold, i.e., $x_M(t)<S_0$. We claim that for the LIFM all firings initiated within $[0,T]$ necessarily stop before t^*. Indeed, let us assume that there is a firing at some initial s in $[0,T]$; then we need to consider the solution $V(t)$ going through V_0 at this time, i.e., $V(s)=V_0$. We show that $V(t)<x_M(t)$ for all $t\geqslant s$, which in turn implies that $V(t)<S_0$ for all $t>t^*$, meaning that no firing can take place after t^*.

To see this point, let us consider the solution $x(t)$ of Eq. (4) satisfying $x(s)=V_0$. Then $x(t)=V(t)$ for t in $[s,s')$, where s' is the first threshold crossing of x (if it exists, otherwise $s'=\infty$). Since $V_0<S_0<x_M(s)$, we have $x(t)<x_M(t)$ for all $t\geqslant s$. Therefore, $x(t)$ [and consequently $V(t)$] can cross the threshold only at a time $s'>s$ such that $x_M(s')>S_0$. After this crossing $V(t)$ no longer coincides with $x(t)$, but rather with the solution $x'(t)$ of Eq. (4) satisfying $x'(s')=V_0$. Hence this solution also satisfies $x'(t)<x_M(t)$ for all $t>s'$. This finishes the proof, as it implies that any solution of Eq. (1) going through V_0 at some time s in $[0,T]$ satisfies $V(t)<x_M(t)$ for all $t>s$.

These three regions exhaust all possibilities for the periodically forced LIFM. When the forcing is sinusoidal, they coincide with the regions described in [3]. Our interest was in the possibility for the LIFM to display locked firing with different rotation numbers for given parameter sets. Clearly, this is impossible in the third region, because for such a selection of parameters the LIFM cannot sustain maintained firing, and this is independent of the initial conditions. In the

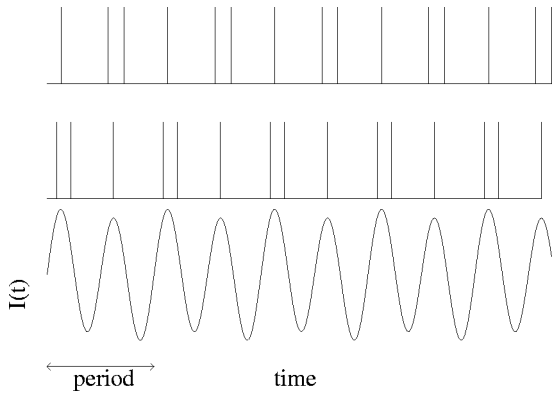

FIG. 2. Example of multistability. Top two graphs are representations of two possible spike trains evoked by the input signal $I(t)$ represented in the bottom panel. The vertical lines in the two upper panels are schematic representations of the firings of the unit. Bottom graph is a schematic representation of the input signal $I(t)$ in arbitrary units. Abscissas of all graphs are time (arbitrary units).

two other regions, the discharge phase map f_c can be restricted to an orientation preserving circle map, which can be either invertible or not. Direct extension of standard results on circle maps [5] reveals that in both cases, i.e., whether the map is invertible or not, the rotation number is well defined, and is independent of the initial condition. Furthermore, the map has a periodic orbit if and only if the rotation number is rational, in which case all periodic orbits have the same period [6]. In other words, the geometrical properties of the map f_c preclude the coexistence of periodic solutions with different rotation numbers, irrespective of the class of periodic inputs selected.

The shape of the map also puts severe constraints on possible dynamics at irrational rotation numbers and also on the size of parameter sets in which these occur [6,7]. When the rotation number is irrational in region 1 where f_c is invertible, one expects quasiperiodic firing, with the orbits of any point densely covering the whole interval $[0,2\pi]$. In contrast, in region 2, the firing is aperiodic and the firing phases form a measure zero Cantor set. The latter case can occur only on a measure zero set of parameters.

Finally, while our analysis proves that no matter what classes of periodic forcing are used, the rotation number does not depend on the initial condition, this does not imply that the periodically forced LIFM does not display multiple stable periodic solutions. Indeed these are possible as long as they have the same rotation number. A schematic example is shown in Fig. 2, where there are two distinct periodic firings with three discharges per input cycle. An example constructed with the LIFM and its corresponding circle map and its third iterate confirm that such a situation can indeed occur (Fig. 3), i.e., the third iterate intersects the diagonal six times at points with slope smaller than 1, indicating the presence of two stable period 3 orbits.

In conclusion, our investigation gives a complete description of the responses of the LIFM to any arbitrary periodic forcing. It also shows that, no matter what class of periodic forcing is used, the LIFM cannot display some of the complex responses, such as chaotic ones, observed in experiments or other models of forced neurons (e.g., [8]). This stems from the fact that the circle map f_c can always be restricted to an orientation preserving map, even though it may display discontinuities. Our proof of this fact did not rely on the explicit expression of the solutions of the LIFM equations; rather it highlighted the two properties of this system that are essential in the results. Indeed, our analysis relied only on the facts that (1) Eq. (4) preserves the order (P1) and (2) it is contractive (P2). This indicates that the results remain valid for any threshold system satisfying these two conditions. Furthermore, condition (P1) holds for all one-dimensional systems, and we used (P2) only in region 2b, so that our analyses of regions 1, 2a, and 3 are valid in fact for arbitrary one-dimensional threshold systems, whether they are contractive or not. These observations stress the generality of our approach, which should also hold for variants of the LIFM with different governing equations.

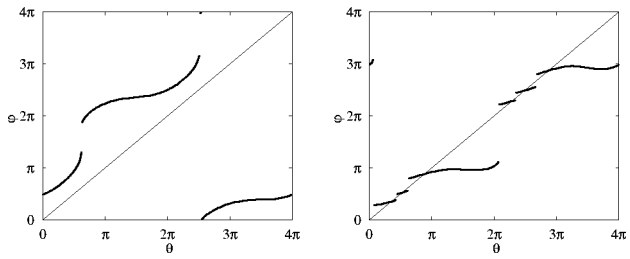

FIG. 3. Circle maps $\varphi = f(\theta)$ (left panel) and $\varphi = f^3(\theta)$ (right panel), associated to the input $I(t) = A\sin(2\pi t + \theta) + 0.1A\sin(\pi t + 0.5\theta)$. Abscissas and ordinates in both panels are in radians. Parameters: $\mu = 2$, $\tau = 1$, $A = 2.5$.

Finally, we illustrate this through a mathematical model for a stretch receptor neuron proposed in [9]. The following is a concise description of this model. In stretch receptor neurons, the stimulation consists in modulating the length of muscle fibers. Such mechanical inputs are transformed into a synaptic current at the level of the neuron membrane thanks to mechanosensitive channels whose opening probability depends on their extension. The standard model for this mechanotransduction process consists in a linear spring with constant k_1 in parallel with a dashpot with viscosity B, which are both in series with a nonlinear spring with constant k_2. The opening of the channels is a function of the extension of this second spring.

Denoting by ϵ the mechanical input and ϵ_2 the extension of the nonlinear spring, we have [9]

$$B\frac{d\epsilon_2}{dt} = -k_1\epsilon_2 - k_2\epsilon_2^{n+1} + k_1\epsilon + B\frac{d\epsilon}{dt}, \tag{9}$$

where the integer n reflects the nonlinearity of the spring. An extension ϵ_2 opens mechanosensitive channels with a probability

$$P_0(\epsilon_2) = \frac{1}{1 + k_b\exp[-(s/m)k_2\epsilon_2^{n+1}]}, \tag{10}$$

where the parameters k_b, s, and m are positive constants. In this way, the synaptic current impinging upon the neuron

membrane can be evaluated as $I_s = g_s P_0(\epsilon_2)(V_s - V)$, where g_s and V_s are the maximal synaptic conductance and the synaptic reversal potential. Combining this result with the LIF gives the following model for stretch receptor neurons:

$$\frac{dV}{dt} = \begin{cases} -\frac{V}{\tau} + \mu + \frac{1}{C} I_s(t) & \text{if } V(t) < S_0 \\ -\left[\frac{1}{\tau} + f(t)\right] V + \mu + h(t) & \text{if } V(t) < S_0, \end{cases} \tag{11}$$

$$V(t^+) = V_0 \quad \text{if } V(t) = S_0, \tag{12}$$

where C is the membrane capacitance, $f(t) = g_s P_0[\epsilon_2(t)]/C > 0$, and $h(t) = f(t) V_s$.

Equation (11) is more complex than the standard LIF Eq. (1) because time dependent terms appear not only in the additive term h but also in the multiplicative one $f(t)$. Furthermore, given that Eq. (9) is nonlinear, it is not in general possible to derive an analytical expression for ϵ_2, even when ϵ is a sine function. Thus an analytical approach may be used to study the above model only in some specific cases. However, given that Eq. (11) satisfies properties (P1) and (P2), the results presented in this work can be used to classify the responses of this model to periodic length modulation.

The author would like to thank T. Shimokawa for discussing these results.

[1] A. Rescigno, R. B. Stein, R. L. Purple, and R. E. Popele, Bull. Math. Biophys. **32**, 337 (1970).
[2] B. W. Knight, J. Gen. Physiol. **59**, 503 (1972); C. Ascoli, M. Barbi, S. Chillemi, and D. Petracchi, Biophys. J. **19**, 219 (1977); L. Glass and M. C. Mackey, J. Math. Biol. **7**, 339 (1979); P. Alstrøm, B. Christiansen, and M. T. Levinsen, Phys. Rev. Lett. **61**, 1679 (1988).
[3] J. P. Keener, F. C. Hoppensteadt, and J. Rinzel, SIAM (Soc. Ind. Appl. Math.) J. Appl. Math. **41**, 503 (1981).
[4] S. Coombes and P. C. Bressloff, Phys. Rev. E **60**, 2086 (1999).
[5] E. Coddington and N. Levinson, *Theory of Ordinary Differential Equations* (McGraw-Hill, New York, 1955).
[6] J. P. Keener, Trans. Am. Math. Soc. **261**, 589 (1980).
[7] F. Rhodes and C. L. Thompson, J. London Math. Soc. 2nd Ser. **43**, 156 (1991).
[8] K. Aihara, G. Matsumoto, and Y. Ikegaya, J. Theor. Biol. **109**, 249 (1984); D. T. Kaplan, J. R. Clay, T. Manning, L. Glass, M. R. Guevara, and A. Shrier, Phys. Rev. Lett. **76**, 4074 (1996).
[9] C. Swerup and B. Rydvist, J. Neurophysiol. **76**, 2211 (1996).